



**HAL**  
open science

## The IL-17 pathway intertwines with neurotrophin and TLR/IL-1R pathways since its domain shuffling origin

Shenghui Chen, Huiping Fan, Chenrui Ran, Yun Hong, Huixiong Feng, Zirui Yue, Hao Zhang, Pierre Pontarotti, Anlong Xu, Shengfeng Huang

### ► To cite this version:

Shenghui Chen, Huiping Fan, Chenrui Ran, Yun Hong, Huixiong Feng, et al.. The IL-17 pathway intertwines with neurotrophin and TLR/IL-1R pathways since its domain shuffling origin. Proceedings of the National Academy of Sciences of the United States of America, 2024, 121 (19), pp.e2400903121. 10.1073/pnas.2400903121 . hal-04564576

**HAL Id: hal-04564576**

**<https://hal.science/hal-04564576>**

Submitted on 30 Apr 2024

**HAL** is a multi-disciplinary open access archive for the deposit and dissemination of scientific research documents, whether they are published or not. The documents may come from teaching and research institutions in France or abroad, or from public or private research centers.

L'archive ouverte pluridisciplinaire **HAL**, est destinée au dépôt et à la diffusion de documents scientifiques de niveau recherche, publiés ou non, émanant des établissements d'enseignement et de recherche français ou étrangers, des laboratoires publics ou privés.

1     **The IL-17 Pathway Intertwines with Neurotrophin and TLR/IL-1R**  
2                     **Pathways Since Its Domain Shuffling Origin**

3  
4     Shenghui Chen<sup>a,b</sup>, Huiping Fan<sup>a</sup>, Chenrui Ran<sup>a</sup>, Yun Hong<sup>a</sup>, Huixiong Feng<sup>a</sup>, Zirui Yue<sup>a</sup>,  
5     Hao Zhang<sup>a</sup>, Pierre Pontarotti<sup>c</sup>, Anlong Xu<sup>a,d,\*</sup> and Shengfeng Huang<sup>a,b,\*</sup>

6  
7     <sup>a</sup>State Key Laboratory of Biocontrol, Southern Marine Science and Engineering  
8     Guangdong Laboratory (Zhuhai), Guangdong Key Laboratory of Pharmaceutical  
9     Functional Genes, School of Life Sciences, Sun Yat-sen University, Guangdong, China

10    <sup>b</sup>Laboratory for Marine Biology and Biotechnology, Qingdao Marine Science and  
11    Technology Center, Qingdao, China.

12    <sup>c</sup>Aix Marseille Université, IRD, APHM, MEPHI, IHU Méditerranée Infection, Marseille,  
13    France 2 CNRS, SNC 5039, Marseille, France

14    <sup>d</sup>School of Life Sciences, Beijing University of Chinese Medicine, Beijing, China

15  
16    \*Corresponding author. School of Life Sciences, Sun Yat-sen University, 135 Xingang  
17    West Street, Haizhu District, Guangzhou 510275, Guangdong Province, People's  
18    Republic of China.

19  
20    Email: [lssxal@mail.sysu.edu.cn](mailto:lssxal@mail.sysu.edu.cn) (AX)

21    Email: [hshengf2@mail.sysu.edu.cn](mailto:hshengf2@mail.sysu.edu.cn) (SH)

22  
23

24 **Abstract**

25 The IL-17 pathway displays remarkably diverse functional modes between different  
26 subphyla, classes and even orders, yet its driving factors remain elusive. Here, we  
27 demonstrate that the IL-17 pathway originated through domain shuffling between a  
28 TLR/IL-1R pathway and a neurotrophin-RTK (receptor-tyrosine-kinase) pathway (a  
29 Trunk-Torso pathway). Unlike other new pathways that evolve independently, the  
30 IL-17 pathway remains intertwined with its donor pathways throughout later evolution.  
31 This intertwining not only influenced the gains and losses of domains and components  
32 in the pathway but also drove the diversification of the pathway's functional modes  
33 among animal lineages. For instance, we reveal that the crustacean female sex  
34 hormone (CFSH), a neurotrophin inducing sex differentiation, could interact with  
35 IL-17Rs and thus be classified as true IL-17s. Additionally, the insect  
36 prothoracicotropic hormone (PTTH), a neurotrophin initiating ecdysis in *Drosophila*  
37 by binding to Torso, could bind to IL-17Rs in other insects. Furthermore, IL-17R and  
38 TLR/IL-1R pathways maintain crosstalk in amphioxus and zebrafish. Moreover, the  
39 loss of the Death domain in the pathway adaptor CIKSs dramatically reduced their  
40 abilities to activate NF- $\kappa$ B and AP-1 in amphioxus and zebrafish. Reinstating this  
41 Death domain not only enhanced NF- $\kappa$ B/AP-1 activation but also strengthened  
42 anti-bacterial immunity in zebrafish larvae. This could explain why the mammalian  
43 IL-17 pathway, whose CIKS also lacks Death, is considered a weak signaling activator,  
44 relying on synergies with other pathways. Our findings provide new insights into the  
45 functional diversity of the IL-17 pathway and unveil evolutionary principles that could  
46 govern the pathway and be used to redesign and manipulate it.

47 **Significance statement**

48 The IL-17 pathway exhibits diverse functions between animal subphyla, classes and  
49 even orders, yet what drives this remain elusive. Here, we demonstrate that this  
50 pathway originated at the dawn of eumetazoans through domain shuffling between a  
51 neurotrophin pathway and a TLR/IL-1R pathway. Unlike most new pathways that  
52 evolve independently, the IL-17 pathway remains intertwined with its donor pathways  
53 throughout subsequent evolution. We demonstrate that this intertwining has resulted in  
54 distinct functional modes for the pathways in crustaceans, insects, amphioxus and  
55 vertebrates. Our study not only provides an interesting example of cytokine origination  
56 and evolution, but also unveils crucial evolutionary principles that govern the  
57 functional plasticity of the IL-17 pathway. These principles may be applied to redesign  
58 and manipulate the pathway.

## 59 **Introduction**

60 In mammals, interleukin-17s (IL-17) were initially identified as the major effectors of  
61 T helper 17 (Th17) cells, but it is now evident that IL-17s act as versatile  
62 pro-inflammatory cytokines (1-4). Together with their cognate receptors (IL-17R) and  
63 adapter (CIKS), IL-17s form a signaling pathway crucial for various processes,  
64 including host defense, tissue repair, and the pathogenesis of cancer, inflammation,  
65 autoimmunity, bone diseases and nervous system diseases (3-5).

66 The mammalian IL-17 pathway typically comprises six ligands (IL-17A-F), five  
67 receptors (IL-17RA-E) and one cytoplasmic adapter (CIKS). IL-17 ligands have a  
68 C-terminal cystine knot domain for binding to IL-17Rs, while canonical IL-17Rs have  
69 a pair of extracellular fibronectin-3 domains (hereafter termed as double-FN3) for  
70 binding ligands and an intracellular SEFIR domain for binding adapters. The adapter  
71 CIKS contains a long N-terminal portion and a C-terminal SEFIR domain. While some  
72 IL-17Rs can activate signaling on their own, CIKS is considered the multifunctional  
73 “hub” of IL-17R signaling (6-9). CIKS contains various functional motifs, especially  
74 in its long N-terminal portion, including RNA-binding sites, TRAF binding sites, and a  
75 U-box with E3 ubiquitin ligase activity for TRAFs. During signaling, IL-17Rs recruit  
76 CIKS through SEFIR-SEFIR interactions, and CIKS recruits TRAF6, leading to the  
77 K63-ubiquitination of TRAF6 and subsequent activation of NF- $\kappa$ B, AP-1 and C/EBPs  
78 (7-9). Besides, CIKS promotes mRNA stability by directly interacting with target  
79 mRNAs or by recruiting TRAF2/5 to mobilize other RNA-binding proteins (9-11).

80 Despite playing prominent roles at the physiological level, the mammalian IL-17  
81 pathway has been considered a weak signaling activator on its own (12-14). Its effects  
82 *in vivo* are believed to be mainly achieved through synergy with other cytokines  
83 (TNF $\alpha$ , IFN $\gamma$ , TGF $\beta$ , IL-1 $\beta$  and IL-13), as well as through crosstalk with other  
84 pathways, including TLRs/IL-1Rs, NOTCH1, TNFRs, EGFRs and FGFRs (14-16).  
85 Due to this unique functional mode, IL-17 has been proposed to be a “chief  
86 orchestrator of immunity” (17). The mechanisms behind the evolution of the IL-17  
87 pathway into this functional mode remain largely unresolved.

88 IL-17 is the only interleukin family conserved in both vertebrates and  
89 invertebrates (18-21). However, there is limited research on the functional aspects of  
90 the IL-17 pathways in lower vertebrates and invertebrates (22-33), and it is unlikely  
91 that they will be explored to the same extent as in mammals in the near future.  
92 Therefore, it is challenging to determine whether the IL-17 pathways in different phyla  
93 follow similar principles, especially if they operate in the same mode as in mammals.

94 There have been long-standing suggestions of structural connections between  
95 IL-17, TLR/IL-1R and neurotrophin/growth factor pathways. For example, both IL-17s  
96 and classic growth factors such as nerve growth factors (NGFs), beta transforming  
97 growth factors (TGF $\beta$ s), and platelet-derived growth factors (PDGFs) have a  
98 C-terminal cystine knot structure (34). Additionally, the SEFIR domains of IL-17Rs  
99 and CIKS, as well as the TIR domain of TLRs/IL-1Rs and their adapters, belong to the  
100 same STIR domain superfamily (35). However, further exploration is needed to  
101 determine whether these pathways contributed to each other's origination.

102 In this study, we investigated the influence of the neurotrophin and TLR/IL-1R  
103 pathways on the IL-17 pathway. Firstly, we conducted a comprehensive phylogenomic  
104 analysis of IL-17-related proteins across major metazoan subphyla. Next, we selected  
105 representative IL-17 pathway components from crustaceans, insects, amphioxus and  
106 zebrafish for functional studies. Our findings suggest that the IL-17 pathway emerged  
107 at the dawn of eumetazoans through domain shuffling between a neurotrophin pathway  
108 and a TLR/IL-1R pathway, and subsequently, it remains intertwined with these  
109 pathways. Furthermore, our study indicates that this origin and intertwining influenced  
110 the structural and compositional evolution of the IL-17 pathway, and led to the  
111 diversification of its functional modes among different animal subphyla, classes and  
112 orders.

## 113 **Results**

### 114 **1. Identification and annotation of IL-17-related sequences**

115 The IL-17/IL-17R/CIKS sequences were identified and annotated using a procedure  
116 established in our previous studies (36, 37). However, we noticed a substantial number  
117 of sequences and domain structures were too divergent to be discovered by this  
118 standard procedure. To uncover them, we employed a sensitive *de novo* method  
119 originally developed to identify novel domains (**see Methods**) (38, 39). The obtained  
120 sequences were grouped into non-redundant clusters and inspected manually. We  
121 curated a collection of representative sequences (**Supplementary Dataset 1**), mainly  
122 focusing on the well-annotated species representing thirteen eumetazoan subphyla (**Fig.**  
123 **1A**).

124 Our data suggest that the IL-17 pathway is present in all thirteen eumetazoan  
125 subphyla but absent in poriferans (the most basal living metazoans) and  
126 choanoflagellates (the closest living relatives of metazoans) (**Fig. 1A**). We also counted  
127 the numbers of non-redundant proteins in each examined species (**Fig. 1A**). The result  
128 shows that most eumetazoan species have two to four IL-17s and IL-17Rs, but there  
129 are exceptions. For instance, amphioxus and some mollusks have over ten IL-17s,  
130 while some arthropods like *Drosophila* have one IL-17 and **no IL-17R**. Regarding  
131 CIKS, most species have one or two genes. However, in echinoderms, arthropods and  
132 annelids, CIKS has not been discovered, even using a sensitive method (**see Methods**).

133

### 134 **2. Sequence divergence and structure variations of the IL-17 pathway**

135 The protein structures of the IL-17 pathway components are highly diversified. The  
136 annotation data allowed us to trace their structural variations along the species tree  
137 (**Fig. 1**). Phylogenetic analyses confirm that the protein sequences of the IL-17  
138 pathway are highly diversified between and within subphyla, with no observed IL-17  
139 or IL-17R orthologs between subphyla (**Fig. S2**), except for CIKS, which remains a  
140 single-copy gene in many species (**Fig. 2A and 2B; Fig. S3**).

141

### 142 **3. Appearance and disappearance of disulfide patterns in IL-17 ligands**

143 IL-17s exhibit little sequence homology, but they all share the cystine knot structure, a  
144 feature also present in many neurotrophins and growth factors (34, 40). This structure  
145 comprises two pairs of  $\beta$ -strands “knotted” by three disulfide bonds from six unusually  
146 positioned cysteines, providing high structural stability and tolerance for sequence  
147 diversity in the  $\beta$ -strands (40-42). Our annotation data reveal that IL-17 cystine knots  
148 can be classified into five structural types (T1A/B/C, T2, and T3), based on their  
149 disulfide patterns and 3D structures (**Fig. 1B-C; Fig. S1**). T1A is the ancestral type,  
150 possessing all three disulfides (cysteines 1/4, 2/5, and 3/6) that covalently knot four  
151  $\beta$ -strands together. T1B and T1C were derived from T1A by losing one disulfide  
152 (cysteines 2/5 and 3/6, respectively), but the remaining two disulfides still link four  
153  $\beta$ -strands together. T1A/B/C constitute a super-type and represent the most prevalent  
154 cystine knot type, existing in all metazoan taxa but lost in the olfactores (tunicates and  
155 vertebrates) (**Fig. 1A**). In the chordate amphioxus, the T1A/B/C types still exist but the  
156 T2 type first emerges, whereare in tunicates and vertebrates, T1A/B/C have all been  
157 lost and T2 becomes the only existing type (**Fig. 1A**). T2 was derived from T1A by  
158 losing an important disulfide (cysteines 1/4), which leaves two  $\beta$ -strands unbound (**Fig.**  
159 **1B-C**). Therefore, all tunicate and vertebrate IL-17s lack two cysteines to complete the  
160 cystine knot, which, as previously suggested (34), requires compensatory non-covalent  
161 interactions to stabilize the structural conformation. However, T2 is not the only type  
162 of incomplete cystine knots. The T3 type of IL-17s, discovered in cnidarians, also  
163 leaves two  $\beta$ -strands unbound due to the lack of cysteines 5/6 (**Fig. 1B-C**).

164

### 165 **4. Recurrent domain degeneration and acquisition in IL-17 receptors**

166 Typically, IL-17R is defined as a type-I transmembrane receptor with two extracellular  
167 FN3 domains (double-FN3) and an intracellular SEFIR domain. However, many  
168 IL-17Rs exhibit little sequence similarity in these domains. Consistent with this  
169 observation, detecting double-FN3 and SEFIR in many IL-17Rs proves challenging,  
170 even using conserved domain models. To understand the extent of the divergence of



171 IL-17R ectodomains, we defined a double-FN3 as “degenerated” when its  
172 RPS-BLAST bit-score is below 25 (where false positives significantly increase). We  
173 then counted the occurrence of "degenerated" double-FN3 in different subphyla. The  
174 results indicated that about half of IL-17Rs in each subphylum, except for amphioxus,  
175 could be considered to carry a “degenerated” double-FN3 (**Fig. 1A and 1D**). Likewise,  
176 sequence “degeneration” was also frequently observed in the SEFIR domain of  
177 IL-17Rs, though to a lesser extent than the double-FN3. Our analysis also indicated  
178 that domain “degeneration” in IL-17Rs occurred independently in different subphyla,  
179 which may be explained by the subphylum-specific rapid coevolution between  
180 IL-17Rs and their ligands and adapters. Finally, it has been observed that some  
181 IL-17Rs of cnidarians and some IL-17Rs of ambulacrarians (echinoderms and  
182 hemichordates) incorporate EGF and IGSF domains into their FN3-containing  
183 ectodomains, respectively (**Fig. 1A and 1D**). For comparison, EGFs and IGSFs are  
184 also found adjacent to the FN3-containing ectodomains in many receptor-tyrosine  
185 kinases (RTKs).

186

## 187 **5. Repeated domain losses in the adapter CIKSs**

188 We showed that CIKS is a single-copy gene in most species, and its evolution largely  
189 recapitulated the species tree (**Fig. 1A and Fig. 2A**). The prevalent architecture of  
190 CIKS comprises an N-terminal Death domain, a C-terminal SEFIR domain, and a long  
191 middle region with U-box E3 ligase and TRAF binding sites (the T1 type in **Fig. 1E**).  
192 This architecture is conserved from the basal eumetazoan cnidarians to the chordate  
193 amphioxus (**Fig. 1A**), suggesting that it represents the ancestral state. However, we  
194 observed domain losses in CIKS proteins from several animal clades (**Fig. 1A and Fig.**  
195 **2A; Fig. S3**). First, all vertebrate and tunicate CIKSs lost the N-terminal Death domain  
196 (the T2 type in **Fig. 1E**). Second, one of the two amphioxus CIKSs lost not only the  
197 Death domain but also a large portion of the middle region (the T3 type in **Fig. 1E**).  
198 Third, some CIKS in cnidarians, like hydra, also lost a large part of the middle region  
199 (the T4 type in **Fig. 1E**). Finally, as a unique but most extreme case of domain loss,

200 CIKS is entirely absent in three subphyla, including annelids, arthropods, and  
201 echinoderms.

202

## 203 **6. Structural and phylogenetic evidence for the domain-shuffling origin of IL-17** 204 **pathways**

205 To investigate the origin of the IL-17 pathway, we conducted a comprehensive analysis  
206 of the domain architectures of IL-17 pathways, TLR/IL-1R pathways, RTK pathways,  
207 and cystine-knot neurotrophin/growth factor pathways (**Fig. 3**). In brief, we propose  
208 that after the split of poriferans and eumetazoans and before the radiation of  
209 eumetazoans, the IL-17 pathway originated from an event of domain shuffling that  
210 occurred between an ancient TLR/IL-1R pathway and an ancient cystine-knot  
211 neurotrophin-RTK pathway (most likely a Trunk-Torso pathway) (**Fig. 3A**). We  
212 described the evidence for this hypothesis below.

213 We showed that among those neurotrophin/growth factor families, five of them  
214 adopt the cystine knot structure, including Trunk, Spätzle, NGF, PDGF (including  
215 VEGF), and TGF $\beta$  (**Fig. 3B**). As for the RTK families, five of them have extracellular  
216 double-FN3 domains (occasionally triple-FN3), including Torso, Eph receptor, Insulin  
217 receptor, Tie receptor, and AXL receptor. As for the TIR domain, which has a common  
218 origin with SEFIR (35), it is present in TLRs, IL-1Rs, and their cognate cytoplasmic  
219 adapters, including MyD88, TRIF, TRAM, Mal and SARM.

220 It has been known that IL-17 signaling relies on the interaction between the  
221 cystine knot domain of the ligands and the double-FN3 region of the receptors. Here  
222 we found that Trunk is the only cystine-knot neurotrophin that binds with the  
223 double-FN3-containing RTK (**Fig. 3B**). According to sequence and phylogenetic  
224 analysis, Trunk is an invertebrate-specific neurotrophin, which is conserved from  
225 cnidarians to the chordate amphioxus and is the closest relative of the IL-17 family  
226 (**Fig. 2C; Fig. S5**). Trunk's cognate receptor, Torso, is an RTK containing no other  
227 domains but a double-FN3 in its ectodomain. Therefore, the Trunk-Torso pathway,  
228 which has been well-known for mediating terminal patterning in *Drosophila* (43-45),

229 exhibits the highest similarity to the IL-17 ligand and receptor ectodomains (**Fig. 3B**).

230       There are other indications of domain shuffling between the TLR/IL-1R and  
231 neurotrophin/growth factor pathways. For instance, the fibroblast growth factor (FGF)  
232 pathway and the IL-1/IL-1R pathway share a beta-trefoil domain in the ligands and  
233 double/triple-IGSF domains in the receptor ectodomains but differ in the receptor  
234 cytoplasmic tails (tyrosine kinase versus TIR domain) (**Fig. 3B**). Another example is  
235 the NGF-RTK pathway and the Spätzle-TLR pathway, which both feature a cystine  
236 knot structure in the ligands and N-terminal LRR repeats in the receptor ectodomains  
237 but differ in the receptor cytoplasmic tails (tyrosine kinase versus TIR domain) (**Fig.**  
238 **3B**).

239       Regarding the IL-17 pathway, all its components (IL-17/IL-17R/CIKS) first  
240 appeared in cnidarians (**Fig. 3A**), whereas IL-1R homologs (i.e., IgTIRs), MyD88,  
241 IRAKs, cystine-knot neurotrophins, and FN3-containing RTKs could be traced even  
242 further back to the poriferans. Therefore, following the principle of maximum  
243 parsimony, we hypothesize that the IL-17 pathway originated after poriferans but  
244 before cnidarians, by splicing the receptor ectodomain of a Trunk-Torso pathway to the  
245 receptor cytoplasmic tail of a TLR/IL-1R pathway (**Fig. 3A**). This hypothesis is further  
246 supported by functional evidence from our group and others (discussed below).

247

## 248 **7. IL-17 and neurotrophin pathways functionally intertwined in arthropods**

249 Sequence and phylogenetic analysis suggest that two families of arthropod  
250 neurotrophins, the crustacean female sex hormones (CFSHs) and the  
251 prothoracicotropic hormones (PTTHs), are closer to IL-17 proteins than to Trunk  
252 proteins (**Fig. 2C**). However, the statistical support from phylogenetics is insufficient to  
253 convincingly classify CFSHs and PTTHs as IL-17 members. Therefore, we sought  
254 functional evidence to support such classifications.

255       In crustaceans, CFSHs were reported as neurotrophins in crabs and shrimps,  
256 released by neurosecretory cells in the eyestalk ganglia to induce sex differentiation  
257 and female reproductive organ development (46, 47). However, so far, CFSHs have not

258 been recognized as IL-17 members, nor have their receptors been identified due to high  
259 sequence divergence. In this study, we discovered IL-17Rs in decapods, and found no  
260 other IL-17 homologs except CFSHs in decapods (**Fig. 4**). To verify if IL-17Rs are  
261 receptors for CFSHs, we investigated the interactions between four CFSHs and two  
262 IL-17Rs from white shrimps. Co-IP assays showed that CFSHs physically interacted  
263 with IL-17Rs when co-expressed in mammalian HEK293T cells (**Fig. 5A**). However,  
264 Co-IP assays may produce false positives due to overexpression and protein  
265 denaturation. Therefore, we conducted a controlled Co-IP assay, in which the IL-17  
266 from amphioxus failed to bind to the shrimp IL-17Rs (**Fig. 5A**). We then performed  
267 immunofluorescence subcellular localization assays. When expressed separately in  
268 mammalian HeLa cells, CFSHs were only present in the cytosol, whereas IL-17Rs  
269 were concentrated on the cell surface. When co-expressed, CFSHs were colocalized  
270 with IL-17Rs not only in the cytosol but also clearly on the cell surface, suggesting that  
271 CFSHs can bind to the cell surface IL-17Rs (**Fig. 5C; Fig. S7**). However, these assays  
272 might also create artifacts because both ligands and receptors were co-expressed within  
273 the same cells in these assays. We therefore proceeded to carry out flow cytometry  
274 assays to further verify the ligand-receptor interactions. Recombinant HA-tagged  
275 CFSH1 proteins were purified from bacteria and examined using Western blot (**Fig.**  
276 **S8**). The purified CFSH1 proteins were incubated with the 293T cells transfected with  
277 GFP-tagged IL-17R proteins, and then analyzed by flow cytometry after being stained  
278 with anti-HA antibodies (**Fig. 5E**). The results demonstrated that recombinant CFSH1  
279 specifically bound to their surface IL-17R1 and 2. Controlled assays were performed in  
280 parallel, including replacing shrimp CFSH1 with insect PTTH (from the lygus bug),  
281 but PTTH could not bind to the surface shrimp IL-17R1 (**Fig. 5E**). Taken together,  
282 these findings confirm the interactions between shrimp CFSHs and IL-17Rs.

283 In insects like *Drosophila*, Trunk mediates embryonic terminal patterning and  
284 molting, whereas PTTH mediates light avoidance, molting and metamorphosis (43, 45,  
285 48). Trunk and PTTH are considered related neurotrophins because they both exert  
286 their roles by binding to the same RTK called Torso (43-45, 49). However, unlike

287 Trunk, which is an ancient RTK and conserved in different invertebrate phyla, PTTH is  
288 specific to insects and shown to be clustered with IL-17/CFSH rather than with Trunk  
289 (**Fig. 2C**). Curiously, we identified IL-17Rs in many insect orders but not in dipterans  
290 (e.g., *Drosophila*) and lepidopterans (e.g., silkworms). This observation prompted us to  
291 hypothesize that the loss of IL-17Rs in dipterans and lepidopterans caused their PTTH  
292 to use Torso as the receptor. However, other insects, such as the hemipteran lygus bug  
293 (*Lygus hesperus*), possess IL-17Rs. We, therefore, hypothesized that PTTH may  
294 interact with IL-17Rs in these insects. To test this hypothesis, we selected PTTH and  
295 two IL-17Rs from the lygus bug to carry out Co-IP assays and subcellular localization  
296 assays. With proper controls, these assays indicated lygus PTTH, but not amphioxus  
297 IL-17L1, could bind with both lygus IL-17R1 and 2 (**Fig. 5B and 5D**). Flow cytometry  
298 assays further confirmed that purified recombinant lygus PTTH (Fig. S10) could  
299 specifically bind to the surface lygus IL-17R1 and 2, while recombinant shrimp  
300 CFSH1 could not bind lygus IL-17R1 (**Fig. 5F**). Taken together, these findings are the  
301 evidence that in insects, the PTTH-IL-17R pathway remains intertwined with the  
302 Trunk-Torso pathway.

303

#### 304 **8. Crosstalk between amphioxus IL-17R and TLR/IL-1R pathways**

305 Amphioxus, recognized as the most basal living chordate, possesses thirteen IL-17s  
306 (twice the number in humans), five IL-17Rs and two CIKSs. The T2 structural type of  
307 IL-17s, which includes all vertebrate IL-17s, first emerged in amphioxus (7 genes) (**Fig.**  
308 **1**). Meanwhile, the ancestral structural type (T1A) and two other derived types (T1B/C)  
309 of IL-17s, commonly found in invertebrates but lost in vertebrates, are all preserved in  
310 amphioxus (1/3/2 genes for T1A/B/C, respectively) (**Fig. 1 and Fig. S1**). Additionally,  
311 amphioxus has two CIKSs: one similar to other invertebrate CIKSs, preserving the  
312 Death domain, and the other similar to vertebrate CIKSs, lacking the Death domain  
313 (**Fig. 1**).

314 In terms of molecular functions, Co-IP assays using HEK293T cells suggested  
315 interaction between amphioxus IL-17 ligand IL-17L1 and receptor IL-17R1 (**Fig. S6**).

316 Co-IP assays and luciferase reporter assays also demonstrated that amphioxus IL-17R1  
317 interacted with both CIKS1 and CIKS2, and both CIKS1 and CIKS2 could activate  
318 NF- $\kappa$ B and AP-1 (**Fig. 6A-D**). Moreover, both CIKS1 and CIKS2 could interact with  
319 TRAF6 and enhance subsequent NF- $\kappa$ B activation (**Fig. 6E-G**). These findings suggest  
320 that amphioxus IL-17R1 recruited TRAF6 to activate NF- $\kappa$ B and AP-1 through  
321 CIKS1/2, thus recapitulating the signaling cascade of the mammalian IL-17R pathway  
322 (6, 14).

323 Given that the TLR/IL-1R pathway contributed the receptor cytoplasmic tail and  
324 adapters to the IL-17R pathway, the two pathways could maintain crosstalk in  
325 amphioxus. Through Co-IP assays, we detected physical interactions between TLR1  
326 and CIKS1 (**Fig. 6H**), as well as between IL-17R1 and MyD88 (**Fig. 6I**), indicating  
327 that the receptors of two pathways retain the abilities to recruit each other's cognate  
328 adapters. Furthermore, Co-IP assays and subcellular localization assays revealed  
329 interactions between MyD88 and CIKS1 as well as CIKS2 (**Fig. 6J and Fig. S10**),  
330 meaning that the cognate adapters of the two pathways are capable of direct crosstalk.  
331 Notably, the reporter assays indicated that CIKS1 enhanced the activating effect of  
332 MyD88 on NF- $\kappa$ B, while conversely, CIKS2, lacking a Death domain, exerted an  
333 inhibitory function in this process (**Fig. 6K**).

334 Moreover, IL-1R associated kinases (IRAK) are also key downstream signal  
335 transducers for the TLR/IL-1R-MyD88 pathway (50). Amphioxus preserves two  
336 ancient lineages of IRAKs, Pelle and IRAK4, both shown to be parts of the amphioxus  
337 MyD88-TRAF6 signaling complex (51). We suspected that these IRAKs are also  
338 recruited by CIKS1, through the interactions between their closely-related Death  
339 domains (**Fig. 2B; Fig. S4**). Indeed, Co-IP assays showed that CIKS1 was associated  
340 with Pelle and IRAK4 (**Fig. 6L**). Reporter assays further showed that Pelle and IRAK4  
341 could weaken the activity of CIKS1 when co-expressed in HEK293T cells (**Fig. 6M**),  
342 which agrees with an early observation that amphioxus Pelle and IRAK4 mildly  
343 suppressed MyD88-mediated NF- $\kappa$ B activation (51). Taken together, these findings  
344 showed that TLR, MyD88, Pelle and IRAK4, the cognate signaling components of the

345 TLR/IL-1R pathway, could interact with the amphioxus IL-17R pathway.

346

### 347 **9. Crosstalk between zebrafish IL-17R and TLR/IL-1R pathways**

348 We further investigated the crosstalk between the IL-17R and TLR/IL-1R pathways in  
349 zebrafish (**Fig. 6N**). Zebrafish possess three CIKSs (CIKS1/2a/2b), all of which are  
350 conserved in other cyprinids such as grass carp. Through Co-IP assays, we detected  
351 interactions between TLR4 and three CIKSs (CIKS1/2a/2b) (**Fig. 6O**), as well as  
352 between three IL-17Rs (IL-17R1a/AL/C) and MyD88 (**Fig. 6P**), indicating that the two  
353 zebrafish pathways maintain the capacity to recruit each other's key adapters. Reporter  
354 assays suggested that IL-17RAL had a significant inhibitory effect on  
355 MyD88-mediated NF- $\kappa$ B activation in HEK293T cells (**Fig. 6Q**). This is reminiscent  
356 of an early discovery that mouse IL-17RD could negatively regulate TLR signaling by  
357 interacting with the TLR adapters MyD88, TRIF and Mal (15). Moreover, Co-IP  
358 assays and subcellular localization assays showed that, like amphioxus CIKSs and  
359 MyD88 (**Fig. 6J**), zebrafish CIKSs and MyD88 could also directly interact with each  
360 other (**Fig. 6R and Fig. S11**). Because all zebrafish CIKSs lack the N-terminal Death  
361 domain like amphioxus CIKS2 does, we tested whether zebrafish CIKSs could inhibit  
362 MyD88 activity as amphioxus CIKS2 did. Zebrafish CIKS2a/2b showed some  
363 inhibitory effect (**Fig. 6S**), but not as strong as amphioxus CIKS2 did (**Fig. 6K**).

364

### 365 **10. Loss of the Death domain in CIKS attenuated the direct signaling ability of** 366 **the IL-17R pathway in both amphioxus and zebrafish**

367 Reporter assays indicated that in amphioxus, CIKS2, which lost the N-terminal Death  
368 domain, was much less potent in activating NF- $\kappa$ B and AP-1 compared to CIKS1 and  
369 MyD88 (**Fig. 6C-D**). In fact, amphioxus CIKS1 appeared to be more potent than  
370 MyD88 (**Fig. 6C-D**). We reasoned that amphioxus CIKS1 may be as strong, if not  
371 stronger, a signaling activator than MyD88 because its Death domain can recruit  
372 IRAKs to enhance downstream signaling. Indeed, our previous study demonstrated that  
373 in amphioxus, when MyD88 lost its Death domain, its ability to activate NF- $\kappa$ B was

374 abolished (52). To verify whether the Death domain is essential for the activity of  
375 amphioxus CIKS1 and CIKS2, we created a mutant CIKS1 without the Death domain  
376 and a mutant CIKS2 with the Death domain restored (**Fig. 7A**). Subsequently, we  
377 carried out reporter assays to compare their activity with wild-type CIKS1 and CIKS2.  
378 It revealed that the Death-less CIKS1 lost the ability to activate NF- $\kappa$ B and AP-1.  
379 Conversely, by fusing the Death domain (from CIKS1) to CIKS2, the activity of  
380 CIKS2 in inducing NF- $\kappa$ B and AP-1 could be enhanced by tens to hundreds of times  
381 (**Fig. 7B-C**).

382 The mammalian IL-17 pathway has long been considered a weak activator on its  
383 own (12-14). As a result, it has been proposed as a “chief orchestrator of immunity”  
384 through synergy and crosstalk with many other pathways (14-17). We hypothesized  
385 that the loss of the Death domain in CIKS is one of the main factors contributing to the  
386 attenuation of the direct activity of the IL-17 pathway in mammals and other  
387 vertebrates. In line with this hypothesis, reporter assays conducted in HEK293T cells  
388 revealed that all three zebrafish CIKSs were much less potent than MyD88 in terms of  
389 NF- $\kappa$ B and AP-1 activation (**Fig. 7D-F**). On the other hand, when restoring the Death  
390 domain (from zebrafish MyD88) to these CIKSs (DD-CIKSs), their activating abilities  
391 could be restored and reached an even higher level than MyD88 (**Fig. 7D-F**). However,  
392 these assays were conducted with mammalian cell lines and might produce artifacts.  
393 Therefore, we injected these DD-CIKS constructs into zebrafish embryos and selected  
394 those GFP-labeled, DD-CIKS-expressing embryos for reporter assays (**Fig. 7G**). The  
395 results indicated that in zebrafish embryos, DD-CIKSs exhibited significantly higher  
396 activating abilities than wild-type CIKSs (**Fig. 7H-J**). Finally, we injected CIKS1 and  
397 DD-CIKS1 into zebrafish eggs to see if they could enhance immunity. DD-CIKS1 was  
398 chosen given that among three CIKS genes, it exhibited the most consistent high effect  
399 on NF- $\kappa$ B in both HEK293T cells and embryos. Forty-eight hours later, we infected  
400 the embryos by puncturing the egg yolk with live bacteria (*Vibrio anguillarum*).  
401 Subsequent observation indicated that GFP-labeled, DD-CIKS1-expressing larvae  
402 exhibited consistently higher survival rates than those expressing wild-type CIKS1



403 (Fig. 7K; Fig. S12). These results reveal that reinstating the Death domain to CIKS1  
404 enhanced not only the signaling ability but also the anti-bacterial immunity in zebrafish  
405 larvae. Taken together, our findings suggest that the loss of the Death domain in CIKS  
406 attenuated the direct activating ability of the vertebrate IL-17 pathway.  
407

## 408 **Discussion**

### 409 **1. The origin and evolution of the IL-17 pathway influenced by neurotrophin and** 410 **TLR/IL-1R pathways**

411 In this study, we presented structural, phylogenomic and functional evidence  
412 supporting the idea that the IL-17 pathway originated at the dawn of eumetazoans  
413 through domain shuffling between a TLR/IL-1R pathway and a Trunk-Torso-like  
414 cystine-knot neurotrophin-RTK pathway (**Fig. 3A**). In line with this, multicellularity at  
415 this era is believed to be accompanied by the assembly of many novel intercellular  
416 signaling proteins through domain shuffling (53-55). Besides, there are two other  
417 possible instances of domain shuffling related to TLRs/IL-1Rs and cystine knot  
418 neurotrophins, one involving the NGF-RTK and Spätzle-TLR pathways, and the other  
419 involving the FGF-FGFR and IL-1-IL-1R pathways (**Fig. 3B**). These four derived  
420 pathways appear to have evolved independently after their emergence. In contrast, the  
421 evolution of the IL-17 pathway appears to have been continuously intertwined with its  
422 donor pathways. For example, here we showed that in arthropods, CFSH and PTTH  
423 were closer to IL-17s and capable of binding with IL-17Rs. In *Drosophila*, however,  
424 PTTH actually signals through binding with Torso, the cognate RTK receptor of the  
425 Trunk-Torso pathway (45). Moreover, in both amphioxus and zebrafish, the IL-17R  
426 pathway has been shown to maintain crosstalk with the TLR/IL-1R pathway. In line  
427 with this, there have been other studies suggesting crosstalk between the IL-17  
428 pathway and its donor pathways: in *C. elegans*, IL-17s signal through IRAKs, the  
429 downstream signal transducers of TLRs/IL-1Rs (30, 31); in mammals, IL-17RD  
430 inhibits TLR-induced inflammation by interacting with the TLR adapters MyD88,  
431 TRIF and Mal (15).

432

### 433 **2. Neurotrophin and TLR/IL-1R pathways contribute to the structural and** 434 **functional plasticity of the IL-17 pathway**

435 The IL-17 pathway exhibits significant structural diversity both between and within  
436 subphyla (**Fig. 1**). In addition to recurrent domain degeneration, losses and gains, key

437 components have been lost. For instance, the T1A/B/C structural types of IL-17s are  
438 entirely lost in vertebrates and urochordates, CIKS adapters are absent in echinoderms,  
439 annelids and arthropods, and both IL-17Rs and CIKSs are missing in certain insect  
440 orders such as *Diptera* and *Lepidoptera*. Viewed from a different perspective, this  
441 structural diversity may reflect functional plasticity. First, the cystine-knot structure is  
442 known for its ability to tolerate significant diversity in its  $\beta$ -strands (40-42), enabling  
443 cystine-knot neurotrophins to bind with very different receptor structures, such as NGF  
444 signaling through both the RTK TrkA and the tumor necrosis factor receptor NGFR. In  
445 this sense, it may not be surprising to observe that insect PTTHs could interact with  
446 both IL-17R and RTK Torso, especially given that both Torso and IL-17R adopt a  
447 similar double-FN3 ectodomain structure, and the Trunk-Torso pathway is presumed to  
448 be a donor pathway for the IL-17 pathway (**Fig. 3**). Second, the sharing of intracellular  
449 adapters between the IL-17 pathway and the TLR/IL-1R pathway could relax purifying  
450 selection, enabling the IL-17 pathway to tolerate domain losses or even component  
451 losses. For example, the direct signaling activity of the vertebrate IL-17R pathway was  
452 significantly reduced by the loss of the Death domain in CIKS (**Fig. 7**). This reduction  
453 could cause the pathway to rely on synergy with other pathways (14-16), rendering the  
454 pathway into a chief immune “orchestrator” rather than a strong immune “activator”  
455 (17). Another example concerns those animal subphyla (echinoderms, annelids, and  
456 arthropods) absent with CIKS; in these cases, their TLR/IL-1R adapters might play a  
457 crucial role in the IL-17R pathway, but it requires verification. Taken together, we  
458 propose that the intertwining with its donor pathways contribute to the structural and  
459 functional plasticity of the IL-17 pathway.

460

### 461 **3. The diverse physiology of the IL-17 pathway related to neurotrophin and** 462 **TLR/IL-1R pathways**

463 The intertwining between the IL-17 pathway and its donor pathways may also  
464 contribute to the diverse physiology of the IL-17 pathway. It is known that classic  
465 cystine knot growth factors, such as NGFs, PDGFs, TGF $\beta$ s, Spätzles and Trunks, can

466 function as important neurotrophins. In line with this, in ecdysozoans, IL-17s appear to  
467 primarily function as neurotrophins. For example, Crustacean CFSHs are released by  
468 neurosecretory cells in the eyestalk ganglia to induce sex differentiation and female  
469 productive phenotypes (46, 47). *Drosophila* PTTH is produced by the brain, promotes  
470 light avoidance, and mediates molting and metamorphosis (43, 45, 48). *C. elegans*  
471 IL-17s are secreted by neurons and modulate sensory responses, escape behaviors,  
472 associative learning, longevity and immunity (30, 31). On the other hand, in mammals,  
473 the IL-17 pathway is mainly considered a key regulator in immunity, including  
474 regulating the activity of its donor pathway, the TLR/IL-1R pathway. However, the  
475 mammalian IL-17 pathway also has diverse non-immune functions in cancer, bone  
476 diseases and the nervous system diseases, such as neurodegeneration, depression and  
477 autism (3-9). In mammals, the IL-17R pathway also promotes other growth factor  
478 pathways, such as EGFR, FGFR, and NOTCH1, through crosstalk with them (9).

479

#### 480 **4. Concluding remarks**

481 Currently, the diverse canonical and non-canonical functions of the IL-17 pathway are  
482 under intense study both in mammals and various non-mammal species. In this study,  
483 we have unveiled crucial evolutionary principles that could govern the functional  
484 plasticity and diversity of the IL-17 pathway, as observed among different animal  
485 subphyla, classes, and even orders. In addition to offering a new framework for  
486 understanding and investigating the functions of the IL-17 pathway, these evolutionary  
487 principles could be employed to control and redesign the pathway for potential  
488 applications.

## 489 **Materials and Methods**

490 A comprehensive search for metazoan IL-17-related sequences was conducted on  
491 NCBI NR and TSA\_NR databases, using the standard homology-based procedure as  
492 described (36, 37), with modifications. A more sensitive, in-house *de novo* method  
493 developed for identifying novel domains (38, 39) was employed to recover extremely  
494 divergent sequences. Retrieved sequences were manually curated before phylogenetic  
495 inference, structural prediction and other bioinformatic analyses. Sequences encoding  
496 IL-17-related proteins were cloned or synthesized from lygus bug *Lygus Hesperus*,  
497 shrimp *Penaeus vannamei*, amphioxus *Branchiostoma belcheri* and zebrafish *Danio*  
498 *rerio*. Interactions between recombinant ligands, receptors and adaptors were analyzed  
499 using human cell lines with Co-immunoprecipitation assays, subcellular  
500 co-localization immunofluorescence assays and flow cytometry assays. Activities  
501 between interacting receptors and adaptors were assessed by luciferase reporter assays  
502 in either human cell lines or zebrafish embryos. The effects of zebrafish CIKS1 with  
503 the reinstated Death domain on antibacterial immunity were evaluated using transient  
504 transgenic zebrafish larvae. For details on materials and methods, see *SI Materials and*  
505 *Methods*.

## 506 Reference

- 507 1. Rouvier E, Luciani MF, Mattéi MG, Denizot F, & Golstein P (1993) CTLA-8,  
508 cloned from an activated T cell, bearing AU-rich messenger RNA instability sequences,  
509 and homologous to a herpesvirus saimiri gene. *The Journal of Immunology*  
510 150(12):5445-5456.
- 511 2. Yao Z, *et al.* (1995) Human IL-17: a novel cytokine derived from T cells. *J*  
512 *Immunol* 155(12):5483-5486.
- 513 3. Amatya N, Garg AV, & Gaffen SL (2017) IL-17 Signaling: The Yin and the  
514 Yang. *Trends Immunol* 38(5):310-322.
- 515 4. Pappu R, Rutz S, & Ouyang W (2012) Regulation of epithelial immunity by  
516 IL-17 family cytokines. *Trends Immunol* 33(7):343-349.
- 517 5. Monin L & Gaffen SL (2018) Interleukin 17 Family Cytokines: Signaling  
518 Mechanisms, Biological Activities, and Therapeutic Implications. *Cold Spring Harb*  
519 *Perspect Biol* 10(4).
- 520 6. Maitra A, *et al.* (2007) Distinct functional motifs within the IL-17 receptor  
521 regulate signal transduction and target gene expression. *Proc Natl Acad Sci U S A*  
522 104(18):7506-7511.
- 523 7. Schwandner R, Yamaguchi K, & Cao Z (2000) Requirement of tumor necrosis  
524 factor receptor-associated factor (TRAF)6 in interleukin 17 signal transduction. *J Exp*  
525 *Med* 191(7):1233-1240.
- 526 8. Qian Y, *et al.* (2007) The adaptor Act1 is required for interleukin 17-dependent  
527 signaling associated with autoimmune and inflammatory disease. *Nat Immunol*  
528 8(3):247-256.
- 529 9. Li X, Bechara R, Zhao J, McGeachy MJ, & Gaffen SL (2019) IL-17  
530 receptor-based signaling and implications for disease. *Nat Immunol* 20(12):1594-1602.
- 531 10. Amatya N, *et al.* (2018) IL-17 integrates multiple self-reinforcing,  
532 feed-forward mechanisms through the RNA binding protein Arid5a. *Sci Signal* 11(551).
- 533 11. Herjan T, *et al.* (2018) IL-17-receptor-associated adaptor Act1 directly  
534 stabilizes mRNAs to mediate IL-17 inflammatory signaling. *Nat Immunol*  
535 19(4):354-365.
- 536 12. Gaffen SL (2009) Structure and signalling in the IL-17 receptor family. *Nature*  
537 *Reviews Immunology* 9(8):556-567.
- 538 13. Gu C, Wu L, & Li X (2013) IL-17 family: Cytokines, receptors and signaling.  
539 *Cytokine* 64(2):477-485.
- 540 14. McGeachy MJ, Cua DJ, & Gaffen SL (2019) The IL-17 Family of Cytokines in  
541 Health and Disease. *Immunity* 50(4):892-906.
- 542 15. Mellett M, *et al.* (2015) Orphan receptor IL-17RD regulates Toll-like receptor  
543 signalling via SEFIR/TIR interactions. *Nat Commun* 6:6669.
- 544 16. Chung SH, Ye XQ, & Iwakura Y (2021) Interleukin-17 family members in  
545 health and disease. *Int Immunol* 33(12):723-729.
- 546 17. Veldhoen M (2017) Interleukin 17 is a chief orchestrator of immunity. *Nat*  
547 *Immunol* 18(6):612-621.

- 548 18. Wu B, Jin M, Zhang Y, Wei T, & Bai Z (2011) Evolution of the IL17 receptor  
549 family in chordates: a new subfamily IL17REL. *Immunogenetics* 63(12):835-845.
- 550 19. Huang XD, Zhang H, & He MX (2015) Comparative and Evolutionary  
551 Analysis of the Interleukin 17 Gene Family in Invertebrates. *PLoS One* 10(7):e0132802.
- 552 20. Wu B, Jin M, Gong J, Du X, & Bai Z (2011) Dynamic evolution of CIKS  
553 (TRAF3IP2/Act1) in metazoans. *Dev Comp Immunol* 35(11):1186-1192.
- 554 21. Rosani U, Varotto L, Gerdol M, Pallavicini A, & Venier P (2015) IL-17  
555 signaling components in bivalves: Comparative sequence analysis and involvement in  
556 the immune responses. *Dev Comp Immunol* 52(2):255-268.
- 557 22. Buckley KM, *et al.* (2017) IL17 factors are early regulators in the gut  
558 epithelium during inflammatory response to *Vibrio* in the sea urchin larva. *eLife* 6.
- 559 23. Roberts S, Gueguen Y, de Lorgeril J, & Goetz F (2008) Rapid accumulation of  
560 an interleukin 17 homolog transcript in *Crassostrea gigas* hemocytes following bacterial  
561 exposure. *Dev Comp Immunol* 32(9):1099-1104.
- 562 24. Wu SZ, Huang XD, Li Q, & He MX (2013) Interleukin-17 in pearl oyster  
563 (*Pinctada fucata*): molecular cloning and functional characterization. *Fish Shellfish*  
564 *Immunol* 34(5):1050-1056.
- 565 25. Vizzini A, *et al.* (2015) *Ciona intestinalis* interleukin 17-like genes expression  
566 is upregulated by LPS challenge. *Dev Comp Immunol* 48(1):129-137.
- 567 26. Martin-Gomez L, Villalba A, Carballal MJ, & Abollo E (2014) Cloning and  
568 characterization of neoplasia-related genes in flat oyster *Ostrea edulis*. *Infect Genet Evol*  
569 23:138-149.
- 570 27. Valenzuela-Munoz V & Gallardo-Escarate C (2014) Molecular cloning and  
571 expression of IRAK-4, IL-17 and I-kappaB genes in *Haliotis rufescens* challenged with  
572 *Vibrio anguillarum*. *Fish Shellfish Immunol* 36(2):503-509.
- 573 28. Li J, *et al.* (2014) Genomic characterization and expression analysis of five  
574 novel IL-17 genes in the Pacific oyster, *Crassostrea gigas*. *Fish Shellfish Immunol*  
575 40(2):455-465.
- 576 29. Saco A, Rey-Campos M, Rosani U, Novoa B, & Figueras A (2021) The  
577 Evolution and Diversity of Interleukin-17 Highlight an Expansion in Marine  
578 Invertebrates and Its Conserved Role in Mucosal Immunity. *Frontiers in Immunology*  
579 12(3042).
- 580 30. Flynn SM, *et al.* (2020) MALT-1 mediates IL-17 neural signaling to regulate *C.*  
581 *elegans* behavior, immunity and longevity. *Nat Commun* 11(1):2099.
- 582 31. Chen C, *et al.* (2017) IL-17 is a neuromodulator of *Caenorhabditis elegans*  
583 sensory responses. *Nature* 542(7639):43-48.
- 584 32. Lv Z, *et al.* (2022) IL-17/IL-17 Receptor Pathway-Mediated Inflammatory  
585 Response in *Apostichopus japonicus* Supports the Conserved Functions of Cytokines in  
586 Invertebrates. *J Immunol* 208(2):464-479.
- 587 33. Okamura Y, Kono T, Sakai M, & Hikima JI (2023) Evolutional perspective and  
588 functional characteristics of interleukin-17 in teleosts. *Fish Shellfish Immunol*  
589 132:108496.
- 590 34. Hymowitz SG, *et al.* (2001) IL-17s adopt a cystine knot fold: structure and

591 activity of a novel cytokine, IL-17F, and implications for receptor binding. *EMBO J*  
592 20(19):5332-5341.

593 35. Novatchkova M, Leibbrandt A, Werzowa J, Neubuser A, & Eisenhaber F (2003)  
594 The STIR-domain superfamily in signal transduction, development and immunity.  
595 *Trends Biochem Sci* 28(5):226-229.

596 36. Li Y, *et al.* (2021) Broad distribution, high diversity and ancient origin of the  
597 ApeC-containing proteins. *Mol Phylogenet Evol* 155:107009.

598 37. Huang S, *et al.* (2008) Genomic analysis of the immune gene repertoire of  
599 amphioxus reveals extraordinary innate complexity and diversity. *Genome Res*  
600 18(7):1112-1126.

601 38. Huang G, *et al.* (2014) Two apextrin-like proteins mediate extracellular and  
602 intracellular bacterial recognition in amphioxus. *Proc Natl Acad Sci U S A*  
603 111(37):13469-13474.

604 39. Huang S, *et al.* (2014) Decelerated genome evolution in modern vertebrates  
605 revealed by analysis of multiple lancelet genomes. *Nat Commun* 5:5896.

606 40. Schwarz E (2017) Cystine knot growth factors and their functionally versatile  
607 proregions. *Biological chemistry* 398(12):1295-1308.

608 41. McDonald NQ & Hendrickson WA (1993) A structural superfamily of growth  
609 factors containing a cystine knot motif. *Cell* 73(3):421-424.

610 42. Sun PD & Davies DR (1995) The cystine-knot growth-factor superfamily.  
611 *Annual review of biophysics and biomolecular structure* 24:269-291.

612 43. Rewitz KF, Yamanaka N, Gilbert LI, & O'Connor MB (2009) The insect  
613 neuropeptide PTH activates receptor tyrosine kinase torso to initiate metamorphosis.  
614 *Science* 326(5958):1403-1405.

615 44. Noguti T, *et al.* (1995) Insect prothoracicotropic hormone: a new member of  
616 the vertebrate growth factor superfamily. *FEBS Lett* 376(3):251-256.

617 45. Li WX (2005) Functions and mechanisms of receptor tyrosine kinase Torso  
618 signaling: lessons from *Drosophila* embryonic terminal development. *Dev Dyn*  
619 232(3):656-672.

620 46. Tsutsui N, Kotaka S, Ohira T, & Sakamoto T (2018) Characterization of distinct  
621 ovarian isoform of crustacean female sex hormone in the kuruma prawn *Marsupenaeus*  
622 *japonicus*. *Comp Biochem Physiol A Mol Integr Physiol* 217:7-16.

623 47. Zmora N & Chung JS (2014) A novel hormone is required for the development  
624 of reproductive phenotypes in adult female crabs. *Endocrinology* 155(1):230-239.

625 48. Yamanaka N, *et al.* (2013) Neuroendocrine control of *Drosophila* larval light  
626 preference. *Science* 341(6150):1113-1116.

627 49. Duncan EJ, Johnson TK, Whisstock JC, Warr CG, & Dearden PK (2014)  
628 Capturing embryonic development from metamorphosis: how did the terminal  
629 patterning signalling pathway of *Drosophila* evolve? *Current Opinion in Insect Science*  
630 1:45-51.

631 50. Flannery S & Bowie AG (2010) The interleukin-1 receptor-associated kinases:  
632 critical regulators of innate immune signalling. *Biochem Pharmacol* 80(12):1981-1991.

633 51. Yan X, *et al.* (2020) Functional Variation of IL-1R-Associated Kinases in the



634 Conserved MyD88-TRAF6 Pathway during Evolution. *J Immunol* 204(4):832-843.  
635 52. Yuan S, *et al.* (2009) An amphioxus TLR with dynamic embryonic expression  
636 pattern responses to pathogens and activates NF-kappaB pathway via MyD88. *Mol*  
637 *Immunol* 46(11-12):2348-2356.  
638 53. Patthy L (2003) Modular assembly of genes and the evolution of new functions.  
639 *Genetica* 118(2-3):217-231.  
640 54. Itoh M, Nacher JC, Kuma K, Goto S, & Kanehisa M (2007) Evolutionary  
641 history and functional implications of protein domains and their combinations in  
642 eukaryotes. *Genome Biol* 8(6):R121.  
643 55. Patthy L (1999) Genome evolution and the evolution of exon-shuffling — a  
644 review. *Gene* 238(1):103-114.  
645

646 **Acknowledgements**

647 This work was supported by NNSF key program (31930084), national S&T project of  
648 China (2023ZD0405404), Guangdong Outstanding Youth Team Project  
649 (2023B1515040002), Guangdong Laboratory (Zhuhai) Project (SML2021SP304) and  
650 Planning Project of Guangdong (2023B1212060028). We thank Dr. Xinyu Yan, Dr. Jin  
651 Li and Ziqing Lu for providing reagents and technical supports. We thank Prof.  
652 Yonghua Wang and Prof. Dongming Lan from South China University of Technology  
653 for providing supports and discussion.

654

655 **Author contributions:** S.H., A.X. and P.P. designed research. S.C. performed  
656 experiments and analyzed data. H.F., C.R., Y.H., H.F., Z.Y. and H.Z. also conducted  
657 some experiments and analyzed the data. S.H. and S.C. drafted the manuscript. A.X. and  
658 P.P. proofread the manuscript. All authors discussed and agreed on the results and  
659 approved the manuscript.

660

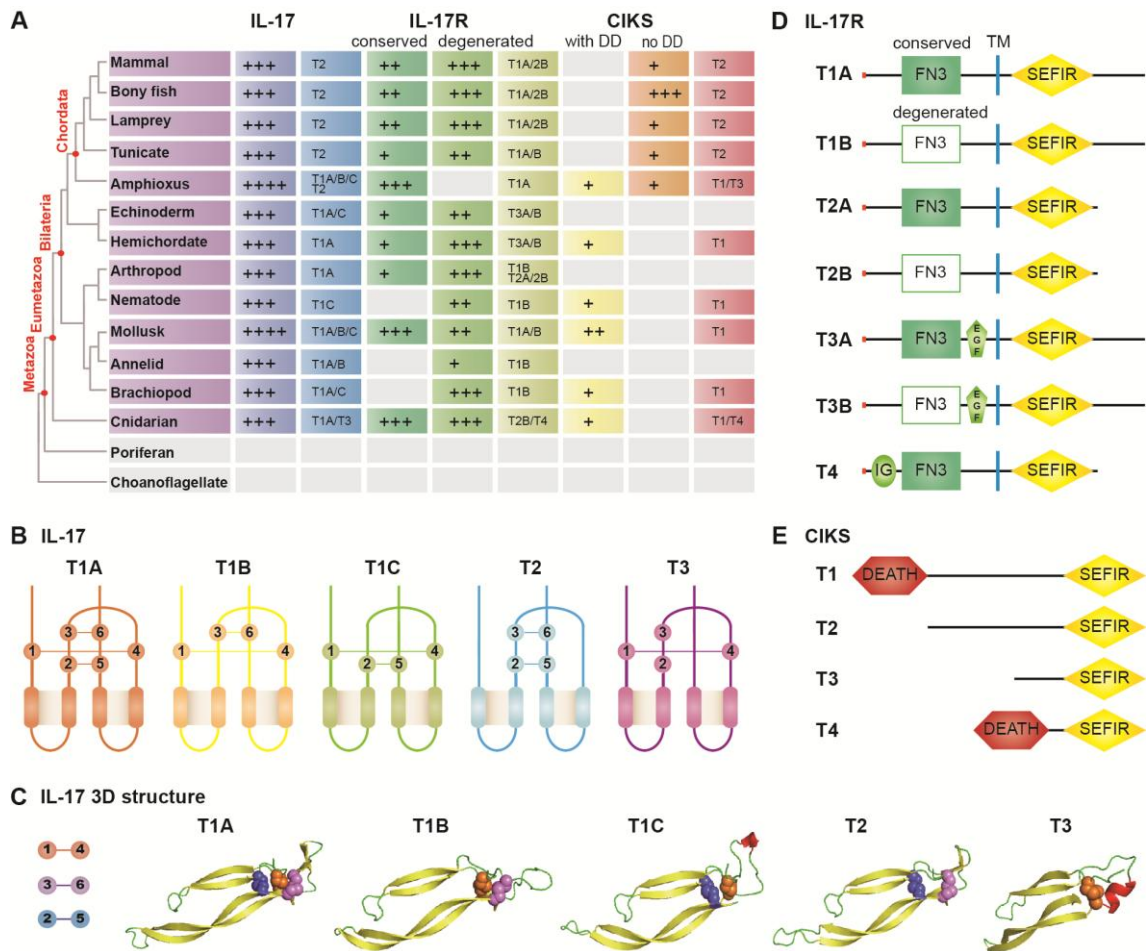
661

662 **Competing interests:** The authors declare no competing interest.

663

664 **Figures**

665 **Figure 1**



666

667 **Figure 1. Compositional and structural diversity of the IL-17 pathway components among**  
 668 **different metazoans.**

669 (A) Distribution of the IL-17 pathway components in different species. Symbols +, ++, +++, +++++  
 670 represent 1, 2, 3-9 and 10+ genes per species, respectively. “Conserved” and “degenerated” IL-17Rs  
 671 contain conserved and extremely diverged FN3 domains, respectively. Grey boxes represent no  
 672 genes found in the species. DD: Death domains.

673 (B) The 2D structures of the cystine-knot domains of different IL-17 types. The balls numbered 1-6  
 674 represented conserved cysteines in the cystine-knot domains. The thin lines indicate the disulfide  
 675 bonds between these cysteines. More details of the structural features are presented in the multiple  
 676 sequence alignment in **Fig. S1**.

677 (C) The 3D structures of different IL-17 types. Three disulfide bonds are shown by balls in different  
 678 colors. Yellow:  $\beta$ -sheet, red:  $\alpha$ -helix, green: random coils.

679 (D) Different architectures of IL-17Rs.

680 (E) Different architectures of adaptor CIKSs.

681 **Figure 2**



682

683 **Figure 2. Phylogenetic analysis of IL-17 and CIKS proteins.**

684 (A) Phylogenetic analysis of CIKSs based on the SEFIR domains.

685 (B) Phylogenetic analysis of CIKSs based on the Death domains.

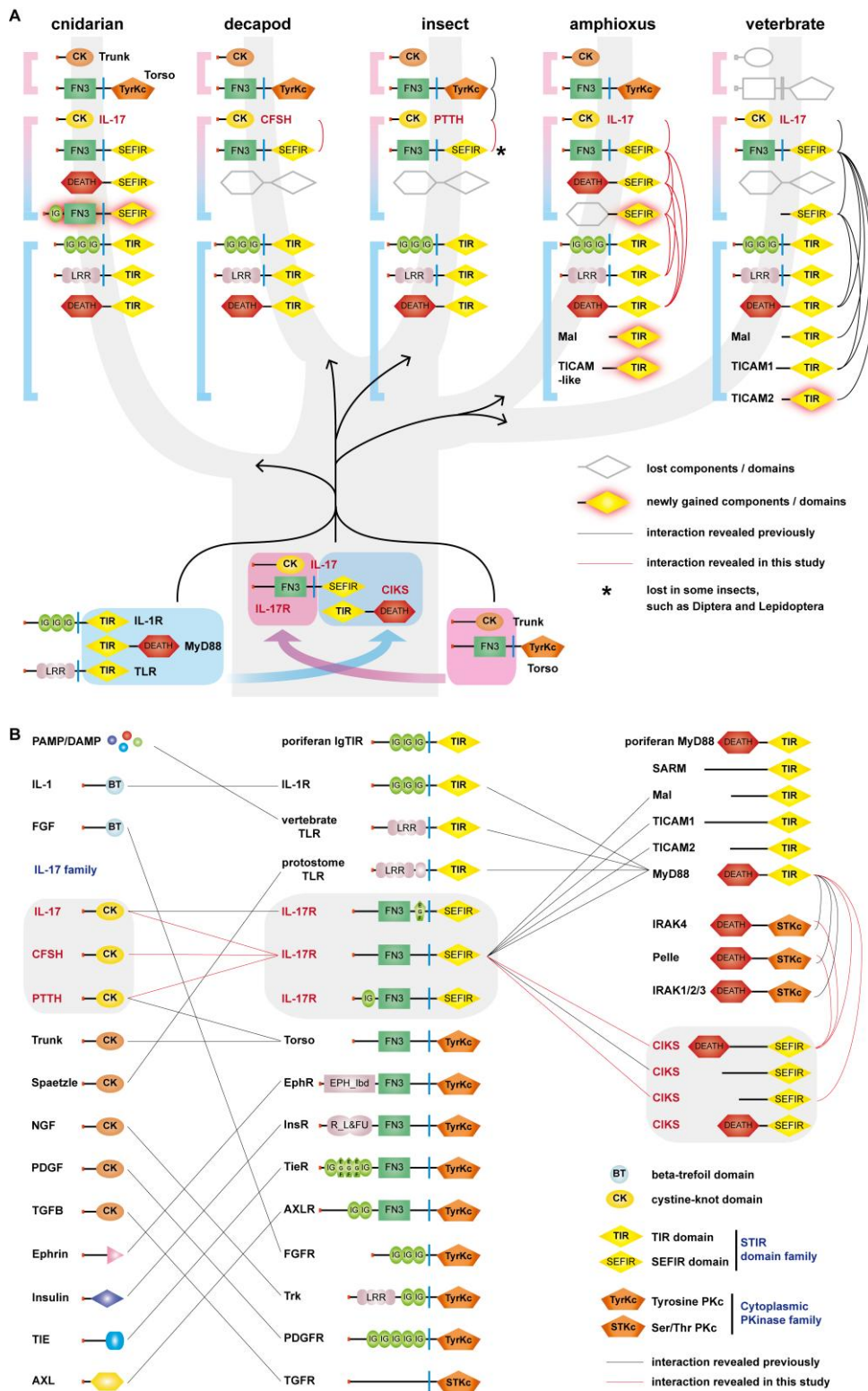
686 (C) Phylogenetic analysis of invertebrate Trunks, PTHs, CFSHs and IL-17s.

687 These trees were constructed using the Maximum Likelihood method (see Methods). The bootstrap

688 values lower than 30 are omitted in the tree. Trees constructed using the Minimum Evolution

689 method are provided in Fig. S3-5. The full species names are given in Tables S3.

690



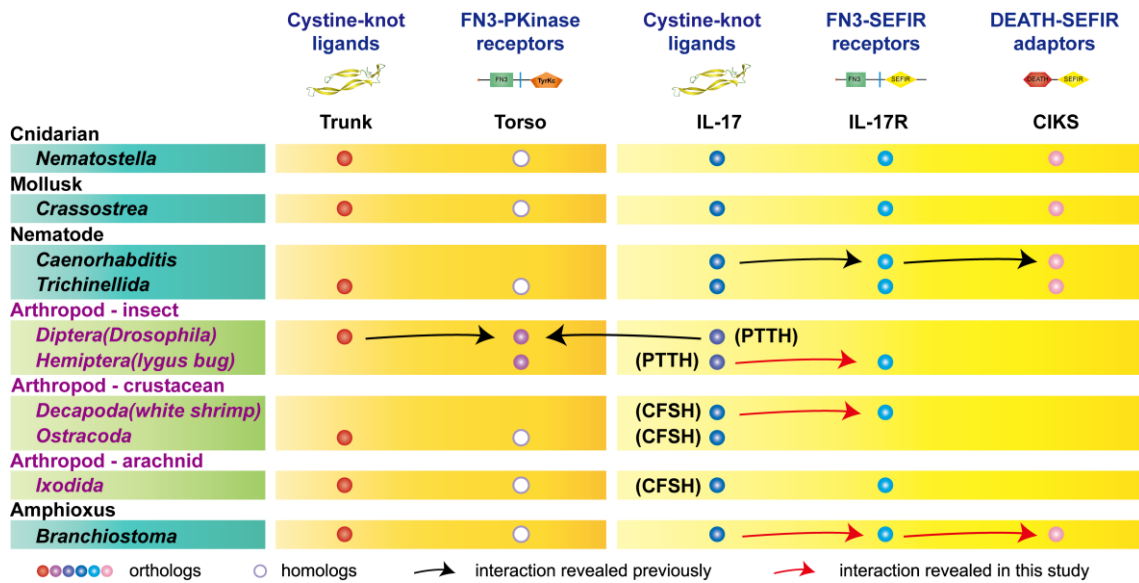
692  
 693 **Figure 3. The relations between the IL-17 pathway, the TLR/IL-1R pathways and the**  
 694 **neurotrophin-RTK pathways**

695 (A) A schematic summarizes the domain-shuffling origin of the IL-17 pathway, the subsequent gains  
 696 and losses of domains and components, and the crosstalk (interactions) with its donor pathways. Five  
 697 animal taxa were chosen as representatives.

698 (B) A schematic shows the similar domain architectures, interactions and crosstalk among IL-17

699 pathways, TLR/IL-1R pathways, the neurotrophin-RTK pathways and other related RTK pathways.  
700 The cystine-knot superfamily of neurotrophins and growth factors include NGFs, TGFs, PDGFs,  
701 Spätzles, Trunks, and IL-17s. The ligands, receptors and adapters of the IL-17 pathway are boxed and  
702 highlighted in red color. Validated interactions are indicated by lines.  
703

704 **Figure 4**



705

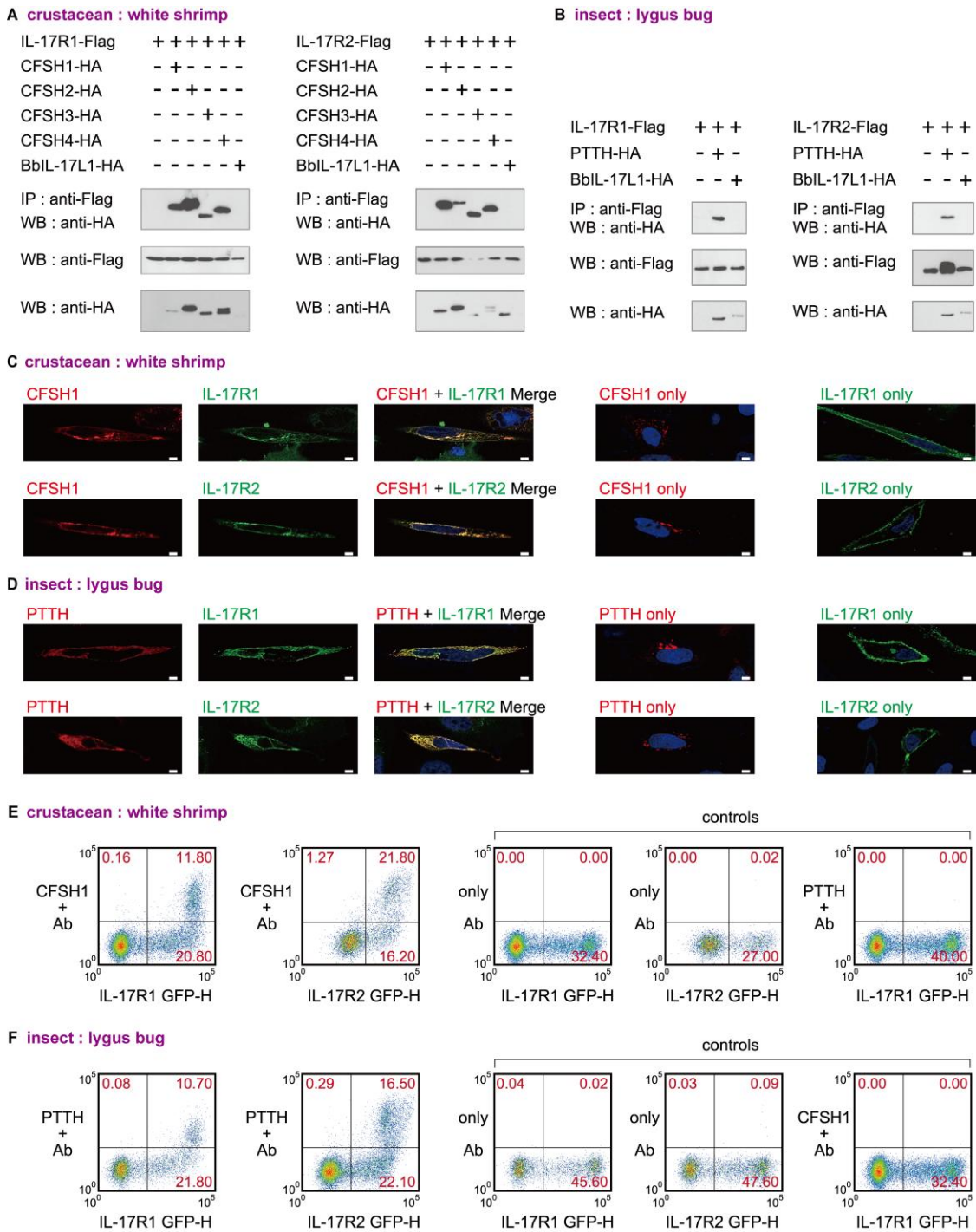
706 **Figure 4. An overview of the presence and absence of the IL-17 pathway components in**  
 707 **cnidarians, mollusks, nematodes, arthropods and amphioxus.**

708 For comparison, Trunk and Torso, the ligand and receptor of an ancient cysteine-knot neurotrophin  
 709 pathway, and the presumed contributors to the extracellular components of the IL-17 pathway, are  
 710 included. The functionally verified interactions between components are either taken from early  
 711 literature (black arrows) or revealed in this study (red arrows). The evidence for the interactions  
 712 between arthropod PTTH, CFSHs and IL-17Rs is presented in **Fig. 5** and **Fig. S7-9**. The evidence for  
 713 the interactions between amphioxus IL-17, IL-17R and CIKS is presented in **Fig. 6** and **Fig. S6**.

714



**Figure 5**



716

717

**Figure 5. The interactions between IL-17 ligands and receptors from shrimps and lygus bugs.**

718

(A-B) Co-IP assays with HEK293T cells were used to assess the interactions between crustacean white shrimp CFSHs and IL-17Rs, and between insect lygus bug PTTH and IL-17Rs. Amphioxus BbIL-17L1 was used as the negative control.

719

720

(C-D) Subcellular colocalization immunofluorescence assays with HeLa cells were used to evaluate the interactions between shrimp CFSH1-mcherry and IL-17R-GFPs, and between lygus bug PTTH-mcherry and IL-17R-GFPs. Transfection with only ligands and receptors served as controls. Additional results for shrimp CFSH2/3/4 were provided in Fig. S7. The scale bar indicated 10 μm.

724

725

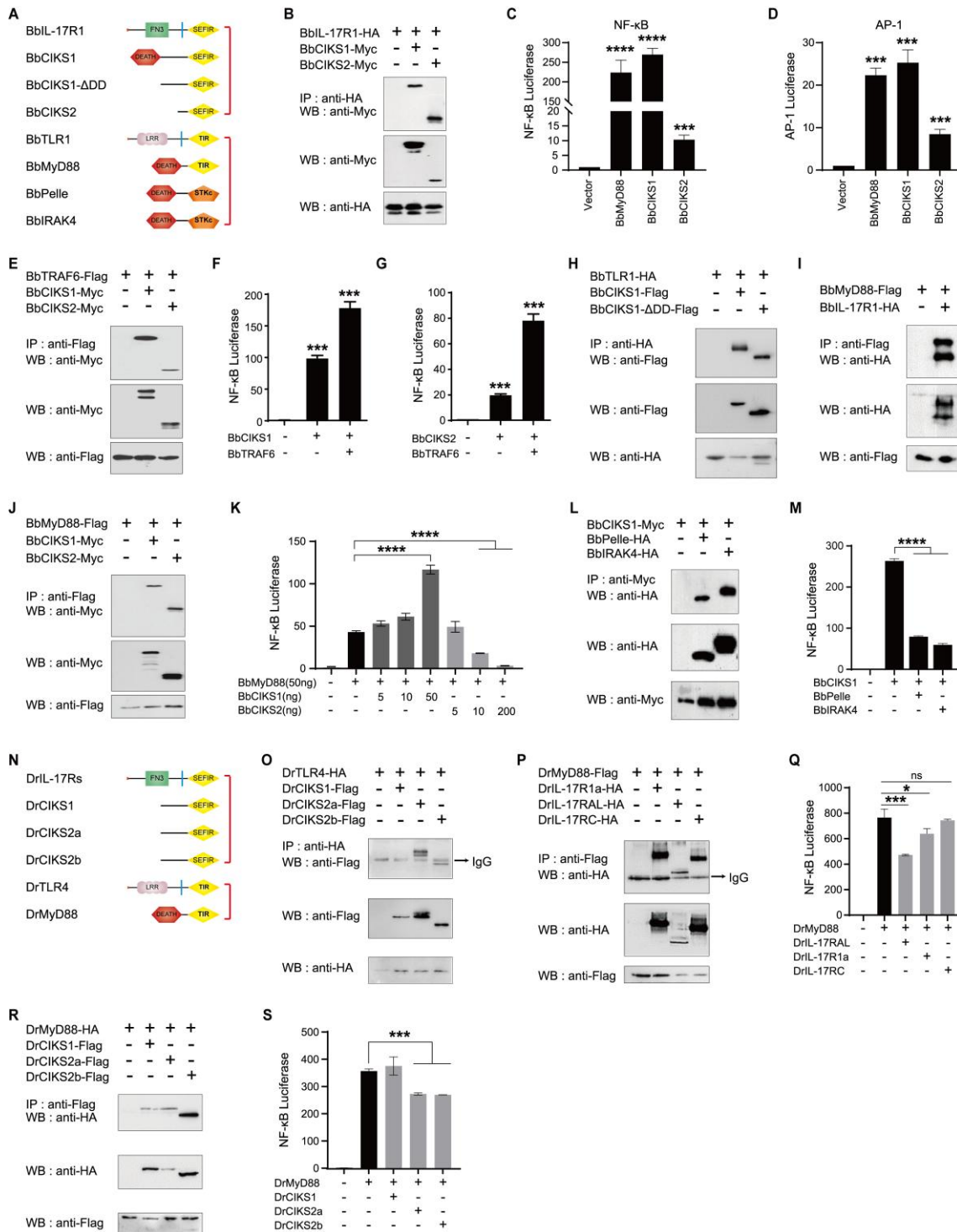
(E-F) Biaxial flow cytometry assays were used to verify the interactions between shrimp CFSH1 and its surface receptors IL-17R1/R2 expressed on HEK293T cells, as well as between lygus bug PTTH

726



727 and its surface receptors IL-17R1/R2 on HEK293T cells. HA-tagged recombinant CFSH1 and PTTH  
728 proteins were extracted from bacteria and examined using Western blot (**Fig. S8-9**). The receptors  
729 were GFP-tagged. Primary antibodies (Ab) are anti-HA monoclonal antibodies. Two types of  
730 controls were conducted: one using the anti-HA antibodies (Ab) only, the other using PTTH and  
731 shrimp CFSH1 as negative controls for shrimp IL-17Rs and lygus IL-17Rs, respectively. The red  
732 number represents the percentage of cells in each gate.  
733

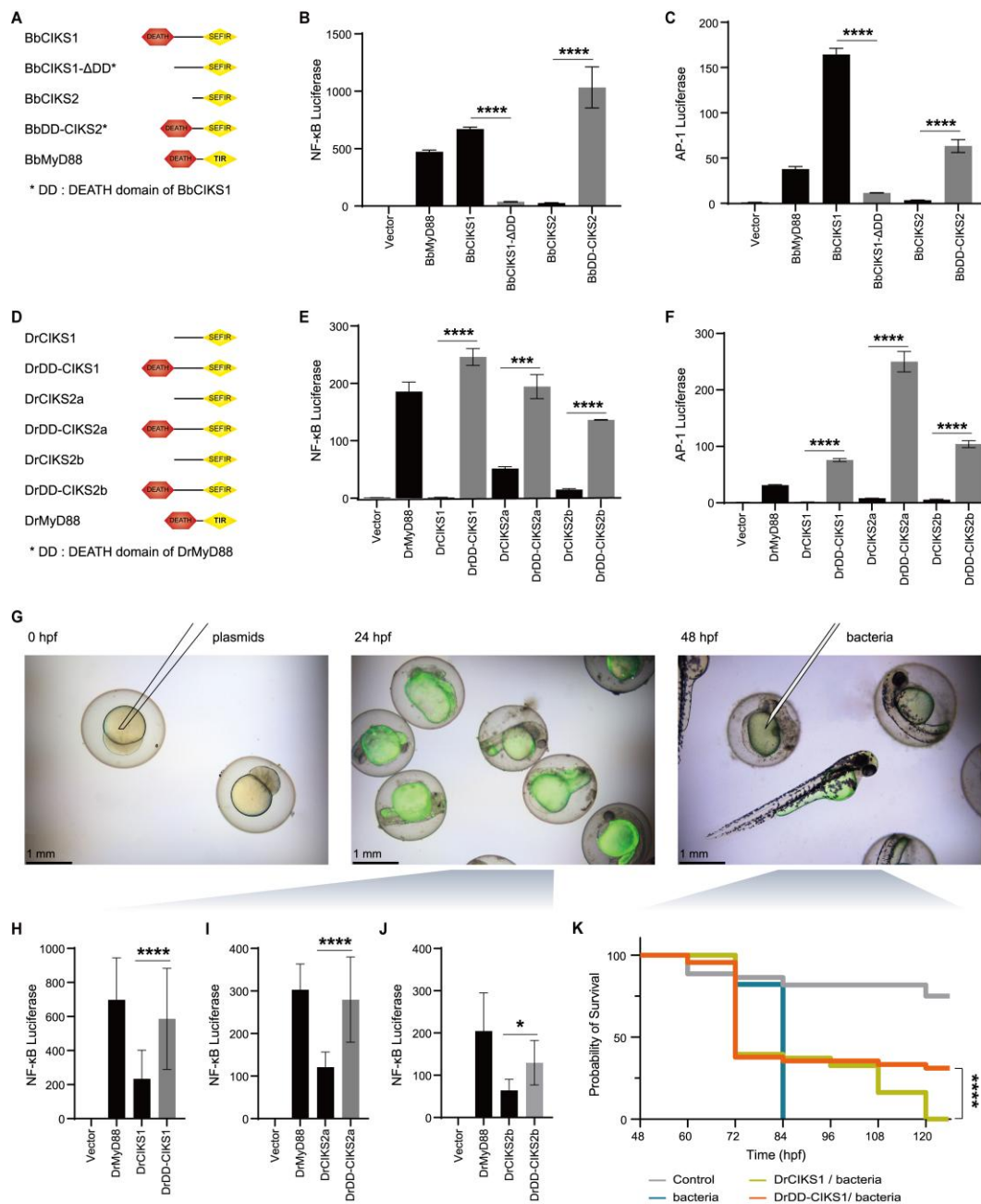
734 **Figure 6**



735 **Figure 6. Crosstalk between the IL-17R and TLR/IL-1R pathways in amphioxus and**  
 736 **zebrafish.**  
 737

738 (A) The constructs used for amphioxus (Bb) proteins.  
 739 (B) Co-IP assays with HEK293T cells were used to analyze the interactions between BbIL-17R1  
 740 and BbCIKSs.  
 741 (C-D) Luciferase reporter assays with HEK293T cells were used to assess the activities of BbCIKSs  
 742 on NF-κB and AP-1 activation.  
 743 (E) The interactions between BbTRAF6 and BbCIKSs.  
 744 (F-G) The activity of BbTRAF6 on the NF-κB activation mediated by BbCIKS1 and by BbCIKS2.

745 (H) The interactions between BbCIKS1/BbCIKS1- $\Delta$ ADD and BbTLR1.  
746 (I) The interactions between BbIL-17R1 and BbMyD88.  
747 (J) The interactions between BbCIKS1/BbCIKS2 and BbMyD88.  
748 (K) The activities of BbCIKS1 on NF- $\kappa$ B activation mediated by BbMyD88.  
749 (L) The interaction between BbCIKS1 with BbPelle and BbIRAK4.  
750 (M) The effects of BbPelle and BbIRAK4 on inhibiting BbCIKS1-mediated NF- $\kappa$ B activation.  
751 (N) The constructs used for zebrafish (Dr) proteins.  
752 (O) Co-IP assays with HEK293T cells were used to analyze the interactions between DrCIKSs and  
753 DrTLR4.  
754 (P) The interactions between DrIL-17Rs and DrMyD88.  
755 (Q) Luciferase reporter assays with HEK293T cells were employed to evaluate the the role of  
756 DrIL-17Rs in NF- $\kappa$ B activation mediated by DrMyD88.  
757 (R) The interactions between DrCIKSs and DrMyD88.  
758 (S) The effects of DrCIKSs on NF- $\kappa$ B activation mediated by DrMyD88.  
759 The protein-protein interactions and NF- $\kappa$ B/AP-1 activation were analyzed by Co-IP and reporter  
760 assays, respectively. Both assays were conducted with HEK293T cells, and each assay was  
761 confirmed by at least three independent experiments. In the reporter assays, 300 ng of the  
762 respective plasmids were transfected into cells if not specified. The reporter results were expressed  
763 as means  $\pm$  SD (n = 3), \*p < 0.05, \*\*p < 0.01, \*\*\*p < 0.001, \*\*\*\*p < 0.0001, ns (p>0.05).



765  
 766 **Figure 7. The loss of the Death domain in CIKSs attenuated the direct activating activity of the**  
 767 **IL-17R pathways in both amphioxus and zebrafish.**  
 768 (A-F) The constructs for amphioxus (Bb) proteins (A-C) and zebrafish (Dr) proteins (D-F) and their  
 769 activities on NF-κB and AP-1 revealed by luciferase reporter assays in HEK293T cells.  
 770 BbDD-CIKS2 was created by fused the Death domain of BbCIKS1 to BbCIKS2. DrDD-CIKSs were  
 771 created by fused the Death domain of DrMyD88 to DrCIKSs. For each construct, 300 ng of plasmids  
 772 were transfected into cells. At least three independent experiments were conducted.  
 773 (G) GFP-tagged adaptor proteins shown in (D) were introduced into zebrafish embryos by  
 774 microinjection at 0 hour post-fertilization (hpf). The 24 hpf GFP-labeled embryos were collected for  
 775 luciferase reporter assays. The 48 hpf GFP-labeled embryos were transferred to a medium containing  
 776 live bacteria *Vibrio anguillarum* (OD600=0.5), punctured with a fine needle in the yolk, and  
 777 monitored of their subsequent survival rates.

778 (H-J) The activities of DrCIKSs and DrDD-CIKSs on NF- $\kappa$ B activation were evaluated by using  
779 luciferase reporter assays in zebrafish embryos The composition of the microinjection systems were  
780 presented in **Table S4**. At least three independent experiments were conducted.

781 (K) The survival rates of zebrafish larvae expressing DrCIKS1 and DrDD-CIKS1 after bacterial  
782 infection were monitored until 120 hpf. Two other independent experiments with slightly different  
783 designs were shown in **Fig. S12**. The specific composition of the injection systems were listed in  
784 **Table S4**.

785 The significance were expressed as: \*p < 0.05, \*\*p < 0.01, \*\*\*p < 0.001, \*\*\*\*p < 0.0001, ns  
786 (p>0.05).

787